Magnetic-field-induced modifications of the electronic structure of $Ni(en)_2NO_2BF_4$: A signature of the Haldane gap in the electronic-excitation intensities

V. C. Long,* Y.-H. Chou, I. A. Cross, A. C. Kozen, J. R. Montague, and E. C. Schundler
Department of Physics and Astronomy, Colby College, Waterville, Maine 04901, USA

X. Wei and S. A. McGill
National High Magnetic Field Laboratory, Tallahassee, Florida 32310, USA

B. R. Landry, K. R. Maxcy-Pearson, and M. M. Turnbull
Carlson School of Chemistry and Biochemistry, Clark University, Worcester, Massachusetts 01060, USA

C. P. Landee
Department of Physics, Clark University, Worcester, Massachusetts 01060, USA
(Received 28 March 2007; published 31 July 2007)

$Ni(en)_2NO_2BF_4$ (NENB) is isostructural to $Ni(en)_2NO_2ClO_4$, the well-known Haldane compound. We have measured the near infrared and visible frequency polarized transmittances of NENB as a function of temperature from 6 to 300 K and in magnetic fields (H) up to 30 T. We identify near infrared spin-allowed and spin-forbidden (SF) *d-d* excitations of the Ni^{2+} ion as well as a Ni^{2+}-to-NO_2^- charge-transfer (CT) transition at 2.5 eV, confirmed by vibrational fine structure on the CT band due to the nitrite ion. The spin-allowed *d-d* bands exhibit temperature dependence consistent with vibronic transitions. The spin-forbidden and electron transfer transitions are noticeably sensitive to magnetic field. Above $H \approx 10$ T, the NENB SF excitation is linearly suppressed by field, whereas the CT transition intensity increases; the onset field agrees with that observed in the high-field magnetization. For comparison, we made the same measurements on a compound having similar near infrared electronic transitions but a different magnetic ground state: the paramagnetic material $Ni(en)_3(ClO_4)_2 \cdot H_2O$ (NEN3P). The SF bands of NENB are relatively more intense than those of NEN3P, suggesting that a spin exchange mechanism enhances their intensity in NENB, in contrast to activation solely by spin-orbit coupling in NEN3P. The H dependence of the SF band also differs in the two materials; in NEN3P, suppression of the SF intensity commences at $H \approx 0$ T. In general, the contrasting behaviors of field-sensitive excitations in the Haldane and paramagnetic analog compounds reveal a correlation between the electronic structure and magnetic properties.

DOI: 10.1103/PhysRevB.76.024439 PACS number(s): 78.20.Ls, 78.40.−q, 78.67.−n

I. INTRODUCTION

In the last two decades, the exotic quantum integer spin chains known as Haldane systems have received much attention from theorists and experimentalists alike, as reviewed recently in Refs. 1–3. The existence of these unique integer spin systems was first conjectured by Haldane,[4] and then validated theoretically by numerical techniques[5,6] and by a valence bond solid model.[7] The predicted spin gap in the magnetic energy spectrum, a signature of the Haldane state, was also confirmed experimentally early on.[8,9] The gap occurs due to quantum spin fluctuations that impede long range order in one dimension, and it separates a correlated spin singlet ground state from the lowest excited spin triplet state.[3] The gap magnitude Δ is directly proportional to the spin exchange, $\Delta = 0.41J$.[5] In molecular Haldane materials, having Ni^{2+} $S=1$ complexes formed into chains by various ligand bridges, the spin gap is generally of the order of 1 meV (Ref. 10) and can therefore be closed by experimentally accessible magnetic fields. The applied field produces Zeeman splitting of the triplet state such that the lowest branch eventually crosses the ground state at a critical field H_C. The closing of the gap at H_C is characterized by the onset of a nonzero magnetization that increases approximately linearly with field,[11–14] consistent with theoretical predictions.[15,16] Other experimental confirmation of the gap comes from electron spin resonance studies[17–22] and neutron scattering.[9,23,24] The latter method is required to observe the substantially larger gap in the linear chain nickelates[25] and other solid state Haldane compounds,[26] in which H_C is inaccessible.

The magnetic properties of the Haldane phase of numerous molecular and solid state Haldane chains are now well characterized,[1,2,10] and the high-field behavior of the molecular materials has also been studied extensively.[18,22,27–36] In addition, the electronic structure of the nickelate Haldane systems has been investigated by optical reflectivity, absorption, and photoemission techniques, with an emphasis on observing the effects of substitutional doping.[37–43] (In these materials, such work is of necessity limited to the spin-gapped state, and the experiments have been carried out in zero field.) In contrast, any manifestation of the Haldane state in the optical properties or electronic structure of the molecular materials has been largely ignored. One exception is an optical birefringence determination of the temperature dependence of the magnetic energy in $Ni(en)_2NO_2ClO_4$ (NENP).[44] On the theoretical side, molecular orbital calculations were used to predict the relative size of the Haldane

gap in a series of molecular Ni^{2+} chain materials.[45] Due to the weak exchange and small spin gap in the molecular compounds, the impact of the Haldane state on the electronic structure is likely to be subtle. The opportunity exists, however, to examine the effect of the high-field phase on the optical properties and thus gain insight into other ramifications of the unique magnetic ground state.

It is the goal of this work to study the correlations between electronic and magnetic ground states in the molecular Haldane Ni^{2+} chain compounds of which NENP is a prototypical system,[9] with particular focus on $Ni(en)_2NO_2BF_4$ (NENB), its close sister compound. NENB and NENP are isostructural,[46–48] both containing Ni^{2+} $S=1$ chains along the *b* axis of the crystal, in the *Pnma* space group. Each Ni^{2+} ion is pseudo-octahedrally coordinated; the four nitrogen atoms of the two ethylenediamine rings (en=ethylenediamine $=C_2N_2H_8$) make approximate square planar symmetry and the NO_2^- groups coordinate via one N and one O atom at the approximate vertices of the octahedron along the chain direction.[46,47,49] The individual chains are well isolated by the inorganic counterions BF_4^- and ClO_4^-; the slightly smaller size of the former counterions in NENB causes slightly greater distortion of the chains, so that the mean planes of successive $Ni(en)_2$ units are canted at about 1° greater angle from each other in NENB.[50] In both NENP and NENB, there exists disorder in the nitrite bridging groups, but the existence of a single Ni^{2+} site in the structural data points to a random distribution of chains with NO_2^- groups ordered along each chain.[46,49,50]

The magnetic properties of NENP have been thoroughly investigated. Magnetic susceptibility measurements on NENP[9,51] yield an antiferromagnetic (*AF*) exchange along the chains $J_\parallel \approx 50$ K, while the ratio of interchain to intrachain exchange[46] $J_\perp/J_\parallel$ is of the order of 10^{-4}. The excellent chain isolation has been confirmed by the absence of long range order down to approximately 0.01 K.[52] When NENP is doped substitutionally at the Ni^{2+} ion sites so that the chains are broken, spin-1/2 degrees of freedom are observed due to the breaking of the "valence bonds" that couple neighboring Ni^{2+} spins.[53,54] Single ion anisotropy in NENP (both axial and rhombic) splits the triplet excited state and produces three distinct spin gaps, with values of 13.6, 15.7, and 29 K, as determined by electron spin resonance.[19] The high-field magnetization likewise yields anisotropic critical fields of 13, 7.5, and 11 T for *H* applied along the *a*, *b*, and *c* axes, respectively.[11] Because the planes of sequential en rings are slightly tilted in opposite directions,[46,49] the Ni^{2+} *g* tensors and magnetic easy planes are also alternately inclined from 90° and the spins experience a staggered transverse field for any finite applied *H*.[55–57] The resulting transverse staggered moment prevents the spin gap from fully closing at H_C and induces a reopening of the gap with increasing field. Thus, no true phase transition takes place,[58] and the field anomaly in the magnetization is more accurately described as a crossover field H_{cr} from low-field to high-field states.[57] Due to the structural similarity of NENP and NENB, the latter's magnetic properties are expected to be virtually identical. There is a report, however, of spin-glass-type behavior in NENB,[59] and there may exist some sample-to-sample variation due to the importance of chain end defects in the magnetic properties, as has also been suggested for NENP.[60–63]

The electronic structure of octahedrally and pseudo-octahedrally coordinated Ni^{2+} ($3d^8$) has been extensively studied and is reviewed in Ref. 64. In octahedral symmetry, the Ni^{2+} ion is in a high spin triplet ground state and has three major spin-allowed *d-d* transitions in the energy range 1–3.5 eV. In such centrosymmetric complexes, the *d-d* transitions are electric-dipole forbidden but can gain intensity through vibronic coupling. Extra structure on the three Ni^{2+} *d-d* bands may be produced by spin-forbidden excitations, vibrational progressions, or low symmetry crystal field effects. The spin-forbidden excitations typically arise from mixing of $S=1$ and $S=0$ spin states by spin-orbit coupling. Charge-transfer transitions involving the Ni^{2+} ion and neighboring ligands are known to occur as well.[64] Early optical studies of NENP and NENB showed essentially identical electronic excitations[47,48] and an unusual spectrum with extra structure and a charge-transfer band attributed to a Ni^{2+}-to-NO_2^- transition.[65,66] Although the low temperature spectrum was analyzed and assigned within an effective C_{4v} symmetry, the temperature-dependent band intensities, which can provide evidence of vibronic activation, were not investigated.[66]

In order to investigate the correlation of magnetic and electronic properties in the molecular Haldane compounds, we have measured the polarized optical transmittance of single crystals of NENB between 1 and 3 eV in an applied magnetic field up to 33 T. We identify the electronic nature of the field-sensitive transitions from further measurements of the low temperature (*T*) and *T*-dependent polarized transmittance at zero magnetic field. For comparison, we made similar studies of some nonchain materials with similar electronic coordination of the (isolated) central Ni^{2+} ions; we refer to the latter as paramagnetic analog compounds. The paper is organized as follows. After reviewing the experimental methods in Sec. II, we report the results of our field-dependent optical studies and high-field magnetization measurements in Secs. III A and III B. In Sec. III C, we report our study of the zero-field electronic structure, which we use to assign the field-sensitive excitations in Sec. III D. To shed further light on the Haldane compound results, we compare them to field-dependent and zero-field measurements on a paramagnetic analog material in Sec. III E. Finally, we discuss possible mechanisms of the field sensitivity in Sec. III F. Our conclusions are summarized in Sec. IV.

II. EXPERIMENTAL MATERIALS AND METHODS

Several batches of single crystals of NENB, NENP, and $Ni(en)_3(ClO_4)_2 \cdot H_2O$ (NEN3P) were synthesized by the following methods. To make NENP, $[Ni(en)_3](ClO_4)_2$ (1.459 g, 3.0 mmol) was dissolved in 6 ml of water. $Ni(ClO_4)_2 \cdot 6H_2O$ (0.609 g, 1.67 mmol) was dissolved separately in 3 ml of water and sodium nitrite (0.346 g, 5.0 mmol) was dissolved in 2 ml of water. The three solutions were combined, stirred, partially covered, and left to evaporate. After one month, the dark red translucent crystals were collected by vacuum filtration, washed with a small amount of cold water, and left to

air dry, giving a final yield of 0.532 g (33%). Samples of NENB were prepared via the same procedure substituting $Ni(BF_4)_2 \cdot 6H_2O$ and $[Ni(en)_3](BF_4)_2$ for the corresponding perchlorate salts. Yields were slightly lower. For NEN3P, $Ni(ClO_4)_2 \cdot 6H_2O$ (16.68 g, 45.6 mmol) was dissolved in 40 ml of water. Ethylenediamine (11.4 ml, 137 mmol) was added with vigorous stirring resulting in a deep purple solution. After several minutes, copious quantities of precipitate formed. The mixture was stirred for 30 min and the solid recovered by vacuum filtration, washed with a small quantity of cold water, and left to air dry, with a yield of 16.14 g (81%). The filtrate was partially covered and left to evaporate slowly in air to produce large translucent purple single crystals of $Ni(en)_3(ClO_4)_2 \cdot H_2O$.

Samples of the Haldane chain compounds were typically needlelike, although a few grew more isotropically. Optical data were confirmed on several samples; the best data are on NENB samples and are reported here. Samples of different thicknesses were used in order to optimize the signal for different types of measurements and different frequency regions of spectra. One very regular shaped NENB crystal of approximate dimensions $6 \times 1.5 \times 1$ mm^3 was used for most of the field-dependent measurements reported here; smaller pieces derived from it, including a very thin platelet with naturally cleaved faces, were also measured. A large polycrystalline NENB sample was deliberately cleaved into many small pieces each of which was an approximate single crystal, several of which were measured, one of which for data shown here. Needlelike crystals of NENP were made into an array for transmittance measurements; others were used individually for field-dependent measurements. Some samples of NEN3P were large and irregular, others were perfect octahedra. To obtain samples thin enough for transmittance measurements, we cleaved small irregular pieces of unknown orientation. Since the structure is nearly cubic,[67] the orientation was irrelevant, and a negligible polarization dependence was confirmed.[68] Since this material is somewhat air sensitive over time (the samples eventually become opaque), we removed the samples from solution and cleaved them shortly before measuring.[69]

We performed temperature-dependent polarized optical transmittance measurements at zero magnetic field using a Bruker IFS 66 V Fourier transform spectrometer over the frequency range 8500–25 000 cm^{-1} (1.05–3.1 eV). A silicon diode detector, tungsten halogen source, and CaF_2 or KBr beam splitters were used in appropriate frequency ranges. The instrument aperture size and number of scans were varied according to the experimental setup and a high pass optical cutoff filter (15 700 cm^{-1}) was used for the higher frequency energy range. A helium-vapor-cooled custom Janis cryostat allowed for excellent temperature (T) control between 6 and 300 K. The signal was optimized using an xy translation stage inserted to the cryostat, and a new reference scan was taken at each temperature. Optical extinction axes, determined by polarization experiments, agreed with our visual assessment of the Haldane sample crystalline axes, assuming the chain axis to be the long axis of the crystal. Polaroid thin film linear polarizers covered the near infrared (NIR) and visible frequency ranges. The NIR polarizer has incomplete polarization between 9500 and 13 000 cm^{-1} (1.18–1.61 eV) and, in the crossed configuration, leaks up to 20% at 11 500 cm^{-1} (1.42 eV), causing some contamination of features from the opposite polarization in the NIR absorption spectrum. Due to a slight horizontal polarization of the spectrometer beam in combination with the polarization leakage, there was also a small sample orientation dependence in the same range.

The measured zero-field transmittance (Tr) was converted to absorption coefficient by $\alpha = -(1/t)\ln(\mathrm{Tr})$, where t is the sample thickness measured with a vernier caliper. This conversion assumes negligible reflectivity,[70] which we confirmed from reflectance measurements on a 1.65 mm thick semiopaque sample of NENB with a good cleaved reflective surface. We found a nearly flat $\approx 3\%$ reflectivity across the NIR and visible regions, which produces a negligible $\approx 1\%$ shift in the recalculated absorption coefficient.[71] However, we found inconsistencies in α for different samples and attribute these to uneven sample thickness, different quality sample surfaces,[72] and the intrinsic uncertainty in measured thickness (error $\approx 10\%$). To account for this type of discrepancy in plots for which different samples were measured in different frequency regions, we have adjusted α by shifting the whole spectrum (subtracting a constant) to match the α value of the less reflective sample. NENB and NENP samples (stored in air) gradually lost some translucency over time. Measurements on the same sample a year or more apart found the transmittance reduced by a large multiplicative constant but no change in the shape of the absorption features; in the absorption data, the change is equivalent to subtracting a constant of up to tens of cm^{-1}. This unexplained change in the otherwise stable samples produces significant uncertainty in our reported absorption coefficient, although the shape and interpretation of the absorption features is unaffected. To follow changes in the NIR or visible absorption intensity with temperature, we calculated the integrated area of the absorption peaks after subtracting a base line. The base line absorption is high and may be partly attributed to the unexplained loss of translucency over time, since many samples were stored for several years. The base line of room temperature middle infrared (MIR) absorption bands[73] is somewhat lower (by 20%–50%), but since we did not measure the T dependence of MIR absorptions, we do not adjust the NIR and visible base lines on that basis. Other contributing factors may include scattering from a poor quality surface in the thicker samples or unaccounted for reflectance from the cleaved faces in thinner samples.

Magnetic field (H) dependence of the optical properties at $T = 4.2$ K was measured using a grating spectrometer, optical fibers, charge coupled device camera, and a sample probe installed in the tail of a helium cryostat inside the bore of a 33 T resistive magnet. Two different sample probe geometries allowed us to align the samples such that the b axis was parallel or perpendicular to the applied magnetic field. In these configurations, the incident light propagated parallel and perpendicular to H, so we identify them as Faraday and Voigt configurations, respectively. We used the same thin film polarizers as in the zero-field measurements and aligned them by eye with the sample edge, giving a probable accuracy within ±10°. Data were taken at magnetic field steps of

1, 2, or 5 T. Since the frequency width of the spectrum is limited by the chosen grating (150 lines/mm), the field step series was repeated in several overlapping spectral regions. The reliability of the absorbance difference features (defined below) was checked by taking a second spectrum at $H=0$ T following the field run and by repeated data collection showing reproducible features.

The field-dependent data were converted to absorbance difference (AD) spectra in order to reveal any small field-induced changes. From the spectrum of single beam intensity I, we calculated the absorbance difference: $\mathrm{AD}=A(H)-A(H=0\ \mathrm{T})=-\ln[I(H)/I(H=0\ \mathrm{T})]$. Since the absorbance difference varies with sample thickness, and we used samples of different thicknesses, we report AD in arbitrary units. In one particular case, the same sample was used for both the H-dependent and zero-field measurements in the same frequency range, and we determined that the absorbance difference features represent a maximum of a 1%–2% change in the low T absorption coefficient.

We took repeated spectra on a number of different NENB and NENP samples, including pieces cleaved from a large polycrystalline sample as well repeated data on different pieces of one very regular shaped NENB sample. Data on different samples were generally consistent. Since the crystalline axes in the polycrystalline-derived samples are not well determined, the only data reported for such a sample are in regions of overlap where the polarized AD features were consistent with those of single crystal data (e.g., above 2.2 eV in Fig. 2). A few AD spectra had inconsistent vertical shifts, and in the case of such inconsistencies, we take the smallest observed change with field to be correct. We found no meaningful difference between the field dependence of the optical properties in the Voigt and Faraday geometries, despite the fact that the direction of applied field varies between the hard axis (Voigt) and the easy plane (Faraday) for the NENB sample. Since the Faraday geometry data are of higher quality and more reproducible, we report only those here. Unpolarized AD spectra taken from two different NEN3P samples were less consistent, although the general feature shapes are similar. The difference may be due to an unrecognized polarization dependence produced by different (unknown) orientations of the irregularly shaped samples.[68]

High-field magnetization measurements were carried out on one single crystal NENB sample (not measured optically) using a vibrating sample magnetometer. The electromagnet was ramped up to 30 T and back down at a rate of 5 T/min, and data were collected approximately every 0.05 T in each direction. The chain direction of the sample was oriented by eye, and the sample was fixed to the holder with GE varnish. The sample was destroyed in the process of removal, so we estimate the mass (accurate to within an order of magnitude) to give an approximate scale for the magnetization.

III. RESULTS AND DISCUSSION

A. Magnetic field dependence of optical absorption spectra

Figure 1 illustrates the magnetic field dependence of the optical absorptions of NENB for polarizations of light parallel (∥) and perpendicular (⊥) to the Ni^{2+} chains in the near

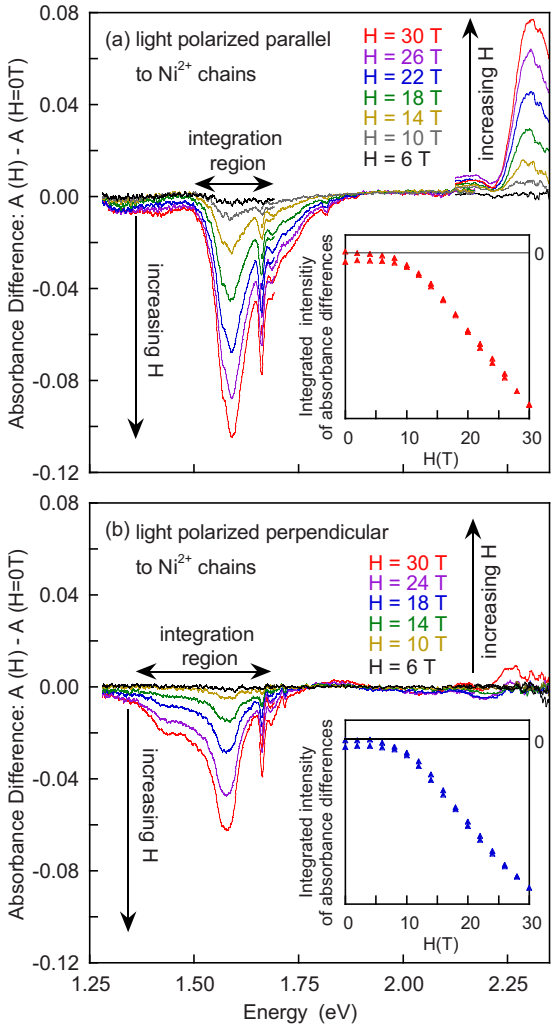

FIG. 1. (Color online) Polarized optical absorbance difference spectra at $T=4.2$ K of single crystal NENB. The absorbance difference (AD) is the absorbance at high magnetic field (H) minus the absorbance at zero field ($H=0$ T). The field was applied parallel to the direction of light propagation (Faraday configuration), and light was polarized either (a) parallel or (b) perpendicular to the Ni^{2+} chains. Three overlapping experimental spectral regions are shown. The spectra are smoothed and shown only at selected field values, which are listed on the figure. The insets show the integrated intensity (area under the curve, calculated from the unsmoothed data) of the absorbance difference as a function of field for the AD features indicated by double arrows. Data were taken at 2 T steps for both increasing and decreasing fields.

infrared (NIR) and lower visible energy ranges between 1.28 and 2.35 eV. [The AD spectra continue to be featureless down to approximately 1.20 eV (not shown).] In the NIR region between about 1.5 and 1.75 eV, the high-field absorbance differences are negative in both polarizations, implying that the material becomes less absorbing with increasing magnetic field in this energy range. Nearly identical AD features appear in both polarizations. The dominant peak is centered at 1.59 (1.57) eV in the parallel (perpendicular) polarization spectrum with an additional broad shoulder on the high (∥) or low (⊥) energy side. A very sharp side feature at 1.66 eV appears identical in both polarizations. The field de-

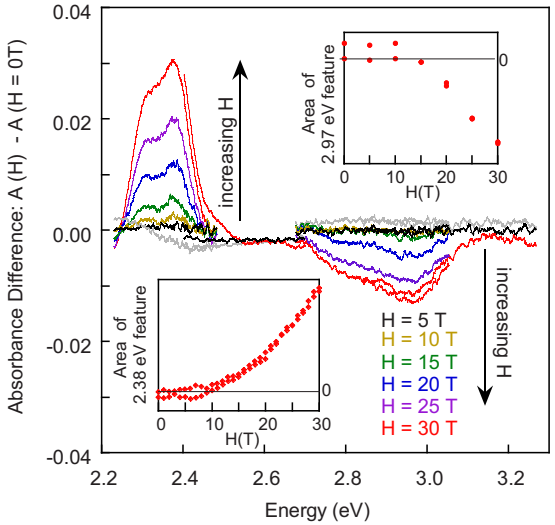

FIG. 2. (Color online) The parallel polarized optical absorbance difference spectra as a function of magnetic field for a sample cleaved from a polycrystal of NENB. The absorbance difference (AD) is the absorbance at high magnetic field (H) minus the absorbance at zero field ($H=0$ T). The field was applied parallel to the direction of light propagation (Faraday configuration). Four overlapping experimental spectral regions are shown. For clarity, the spectra were smoothed and only selected field values (5, 10, 15, 20, 25, and 30 T) are shown, in addition to a final data set taken at zero field, after the field run, shown in light gray. (In regions with no features, only 5 and 30 T spectra are shown; in the 2.97 eV feature, the 5, 10, and 15 T spectra cannot be distinguished.) The insets show the integrated intensity (area under the curve) for the indicated AD feature, with data taken for both increasing and decreasing fields.

pendence of these features is not monotonic, but rather has a distinct onset in the vicinity of $H=10$ T, the same in both polarizations and identical for the individual peaks. As shown in the insets of Fig. 1, which plot the integrated intensity of the absorbance differences versus magnetic field, the intensity decreases approximately linearly with field above the onset field, below which no changes occur.

In contrast to the relative lack of polarization dependence for the NIR AD features, there is a strong polarization effect at higher energy. Figure 1 shows that for light polarized parallel to the Ni^{2+} chains, there is an AD feature that increases with H, centered at approximately 2.3 eV, whereas the perpendicular polarization spectrum exhibits only the most minimal of features at that energy. Figure 2 shows the same feature in parallel polarized light for a different sample. The field dependence of the 2.3 eV AD peak is similar to that of the NIR features, although opposite in sign. The magnitude of intensity changes versus field for this peak is displayed in the lower left inset of Fig. 2, showing that it too has an onset of changes near $H=10$ T. Figure 2 also displays the parallel polarization absorbance differences up to 3.25 eV. An additional AD feature centered around 2.96 eV decreases in intensity with increasing magnetic field. Due to the poorer signal-to-noise ratio in this region, spectra were taken at 5 T intervals, but the field dependence of the integrated intensity (upper inset) still reveals an anomaly in the general vicinity of 10 T.

To summarize, we identify three discrete absorbance difference features, at approximately 1.6, 2.3, and 3.0 eV, each with its own characteristic field dependence that either increases or decreases above an onset field of approximately 10 T. We infer that each AD feature is due to field-induced modifications of a distinct electronic excitation; the excitations will be identified from the temperature-dependent zero-field absorption spectra described in Sec. III C. The AD features of NENB vary only in height, with no shifts in peak energy or changes in basic shape; indeed, each high-field AD spectrum is a nearly perfect multiple of a lower-field spectrum (for field values greater than the onset field). If the electronic-excitation energies were changing with field, we would expect to see derivative-shaped AD features, but none of these occur. We conclude that within our resolution, only the electronic absorption *intensities* of NENB are affected by magnetic field. As remarked earlier, the magnitude of the intensity change is very small relative to the total absorption coefficient α. The maximum change occurs in the parallel polarization; changes in the 1.59 eV feature constitute an approximate 2% decrease in α at $H=30$ T.

The appearance and magnitude of the onset field in the NENB optical properties are strongly reminiscent of the crossover fields $H_{cr}=7-13$ T, observed in magnetization measurements of the Haldane compound NENP.[11,12] NENB is isostructural to NENP[46,50] and thus assumed to be a Haldane system. As will be described in Sec. III B, we confirm the Haldane state in NENB with the observation of a weak field anomaly in the high-field magnetization. We have also verified that the field-dependent results on NENB described above are a result of its Haldane nature and not a peculiarity of other unknown electronic or magnetic properties, from a similar set of field-dependent absorbance difference measurements on NENP. NENP AD spectra exhibit nearly identical features to those of NENB,[74] with only small discrepancies in energy or polarization and with similar onset field behavior in the integrated intensities. A detailed comparison of NENP and NENB in terms of their zero-field and field-modified optical properties reflects small differences in the structures of the two compounds due to different counterions and will be published elsewhere.[75] The comparison supports our hypothesis that the observed changes in electronic spectra of NENB are closely correlated to the Haldane state, so we now interpret them in that context and henceforth identify the onset field of intensity changes with the crossover field H_{cr}.

B. High-field magnetization

Figure 3 shows the high-field magnetization of NENB for H applied both parallel and perpendicular to the Ni^{2+} chains at $T=1.7$ K. Most noticeably, the magnetic moment does not increase monotonically; instead, kinks are observed in $M(H)$ for both orientations of field, as expected for a singlet ground state.[11] The observed field anomalies at 8.6 and 10.0 T in NENB are not as sharp, however, as the same transitions at 7.5 and ~12 T in NENP, although the latter also reveal some broadening, and the perpendicular directions show small finite magnetization at low field.[11,12] In both materials, a broad

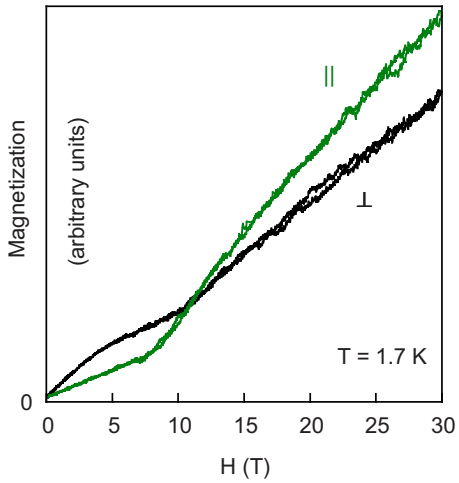

FIG. 3. (Color online) The magnetization M of single crystal NENB is shown in arbitrary units as a function of magnetic field H with the field directed either parallel (||) or perpendicular ($\perp$) to the Ni^{2+} chains. Data were taken for both increasing and decreasing fields. We locate the crossover fields at the kinks in the curves, yielding $H_{cr,\|} \approx 8.6$ T and $H_{cr,\perp} \approx 10.0$ T. The estimated scale of M is of the order of 10^{-1} μ_B per Ni^{2+} atom at $H=30$ T.

crossover can be attributed to the induced transverse staggered moment that arises due to the alternately canted g tensors in an applied uniform field.[55,57] The *greater* broadening and finite magnetization below the transition in NENB might be explained, at least in part, by its slightly greater canting angles.[50] Sakai and Shiba calculated the uniform parallel magnetization for values of the internal staggered field differing by a factor of 3.[57] Although this difference is much greater than that between NENB and NENP, and the scale of Fig. 4 in Ref. 57 precludes any precise determination, more broadening is indeed observed in the system with greater internal staggered field. Another possible contributing factor to the weakness of the magnetization anomalies in NENB is chain end defects. Published magnetic susceptibility experiments on NENB have been suggestive of spin glass behavior in some samples,[59] which might also be accounted for by large numbers of defects. Electron spin resonance measurements on undoped NENB also reveal a significant spin-1/2 signal due to chain ends, along with the usual anisotropic gap.[76] Nevertheless, both the distinct field anomalies in the magnetization and the onset field observed in the field-dependent optical properties seem to be clearly associated with the Haldane state.

C. Electronic structure at zero magnetic field

Figures 4 and 5 show the temperature dependence of electronic excitations in NENB for light polarized parallel and perpendicular to the chains in the near infrared and visible regions, respectively. Since the two frequency regions contain excitations of different electronic nature, we discuss each in turn.

Figure 4 shows the temperature-dependent NIR absorptions of NENB in perpendicular and parallel polarizations of light. Looking first at the lowest T spectra (in black), there

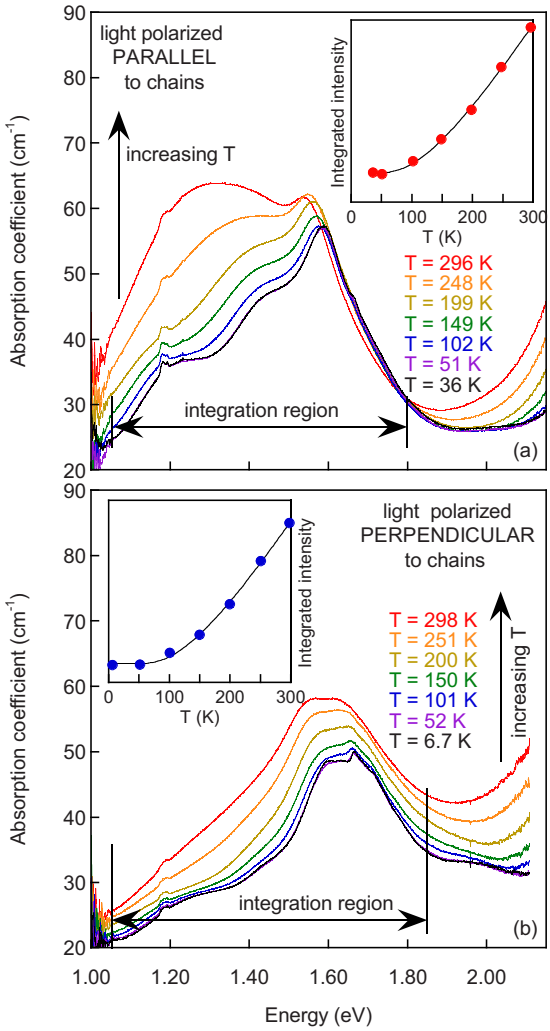

FIG. 4. (Color online) Near infrared zero-field absorption coefficient (α) spectra of single crystal NENB for light polarized (a) parallel (||) and (b) perpendicular ($\perp$) to the Ni^{2+} chains. As discussed in Sec. II, there is large uncertainty in the base line value of α but the shapes of the absorption features are unaffected. Spectra were taken at the temperatures (T) listed on the graph. The two lowest T spectra are nearly identical and cannot be distinguished on this scale. The insets show the integrated intensity versus T of the NIR bands for the integration regions indicated by double arrows. [A base line absorption of 25 cm^{-1} (21 cm^{-1}) was subtracted from the || ($\perp$) polarization spectra before integration.] Solid lines give fits to the expected coth ($h\nu/kT$) dependence for vibronic bands.

are several absorption features common to both polarizations: two rounded bands at approximately 1.23 (1.26) and 1.43 (1.44) eV, a peaked band at 1.58 (1.60) eV, and a tiny sharp shoulder at 1.66 (1.66) eV in the || ($\perp$) polarization. The weak 1.43 eV band in the $\perp$ polarization may be an artifact arising from the strong || polarized band and polarizer leakage at this energy. In the perpendicular polarization, additional structure appears between 1.6 and 1.9 eV, and another broad band occurs at approximately 1.97 eV. The small bump at 1.18 eV in both polarizations is a vibrational mode, likely the second overtone of the N-H_2 stretching vibration. Note that the vertical scale of the plots in Fig. 4 begins at 20 cm^{-1} and the base line absorption is unexpectedly high, as

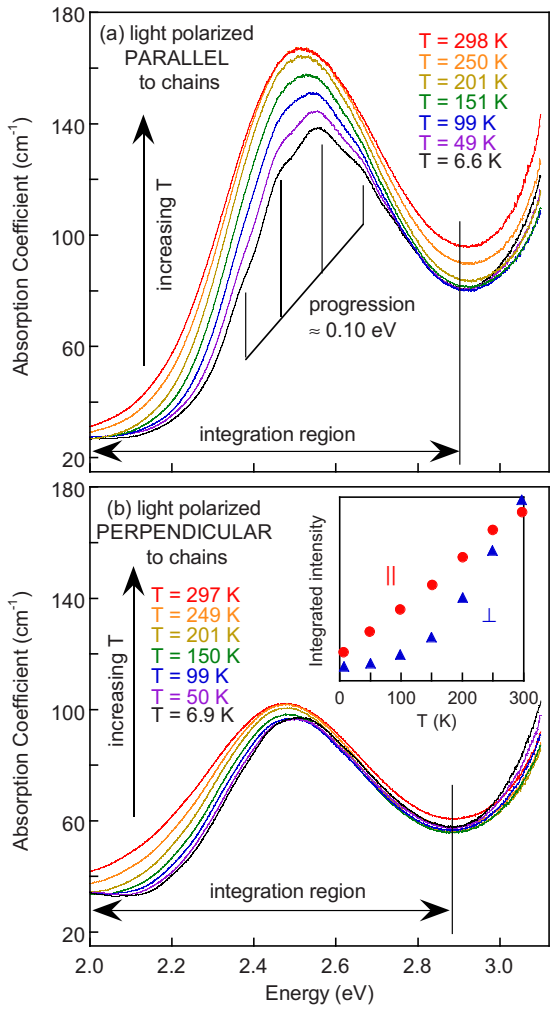

FIG. 5. (Color online) Visible region zero-field absorption coefficient of single crystal NENB for light polarized (a) parallel and (b) perpendicular to the Ni^{2+} chains. The spectra are all shifted vertically downward by a constant, to overlap the spectra of Fig. 4, as discussed in Sec. II. In addition to this shift, the base line value of α is uncertain for reasons also discussed in Sec. II; the shapes of the absorption features are not affected, however. Spectra were taken at the temperatures (T) listed on the graph. The vibrational progression in (a) has separation $\Delta E \approx 0.10$ eV (800 cm^{-1}). The insets show the integrated intensity versus T of the visible absorption bands for the integration regions indicated by double arrows. [A base line absorption of 24 cm^{-1} (32 cm^{-1}) was subtracted from the $\parallel$ ($\perp$) polarization spectra before integration.] The T dependence is significantly weaker than the coth ($h\nu/kT$) function expected for vibronic bands.

mentioned in Sec. II. Although this height is probably largely due to the artifacts discussed in Sec. II, it may also reflect contributions from an underlying T-independent band, obscured by the overlapping T-dependent bands.

The T dependence of the NIR absorptions is quantified in the insets of Fig. 4, which show the integrated intensities of the bands at a series of temperatures after a flat T-independent base line absorption is subtracted. The solid lines are fits to the expected coth($h\nu/kT$) behavior of a vibronic band.[77] We attempted to fit Gaussian band shapes (expected for vibronically induced bands[77]) in order to follow the T dependence of individual bands, but substantial overlap of the bands precluded any accurate band fitting. In principle, the frequency ν of an effective single vibration that couples to a given d-d excitation can be extracted from the coth($h\nu/kT$) fit. In our case, the derived vibrational frequencies are somewhat suspect due to uncertainty about the actual nature and value of the subtracted base line. Our best fits (shown) were made after subtracting absorption coefficient base lines of α=25 cm^{-1} ($\parallel$) and 21 cm^{-1} ($\perp$) over the integration ranges shown, yielding values of $h\nu$=0.032 eV (260 cm^{-1}) for the $\parallel$ polarization and 0.034 eV (280 cm^{-1}) for the $\perp$ polarization. These frequencies are consistent with an observed vibrational mode at 293 cm^{-1} involving Ni bonded to N.[78,79]

Previous optical measurements of NENP and NENB found that the spectra are very similar,[47,48] which we have confirmed.[75,80] A few reports of room temperature diffuse reflectance and low temperature absorbance spectra of NENP have been published,[48,65,66,81] but no detailed study of the temperature dependence of the optical properties has been carried out before this. The most careful study[66] assigned the two primary NIR bands of NENP as the split lowest energy d-d transition within a C_{4v} molecular symmetry; the extra structure was not assigned in detail. We suggest an alternative set of qualitative assignments within an effective D_{4h} molecular symmetry based on the T dependence of the bands and on information gleaned from our H-dependent measurements, as discussed below. As seen in Fig. 4, the low energy broad bands noticeably increase in intensity with temperature, implying that they are vibronically activated; the coth($h\nu/kT$) fits to the integrated intensities confirm a substantial vibronic component to these bands. Although the actual molecular symmetry of the Ni^{2+} complex is C_1, an effective C_{4v} symmetry, previously suggested,[66] reflects the nearly square configuration of the ethylene diamine rings around the central Ni^{2+} ion as well as the lack of inversion center due to different coordinations of the nitrite group. However, group theory predictions for d-d transitions in C_{4v} symmetry include an electric-dipole-allowed $^3B_1$-to-^3E transition and greater intensity for transitions that are perpendicularly polarized,[82] none of which we observe. In contrast, for an effective centrosymmetric D_{4h} symmetry, all spin-allowed bands are forbidden and must be vibronically induced. Such a scenario is in better agreement with our NIR data of NENB, although a possible underlying T-independent component would be consistent with an aspect of lower actual symmetry.

We assign the two lowest energy broad bands, at approximately 1.2 and 1.4 eV, as spin-allowed excitations to a pair of levels (^3E_g and $^3B_{2g}$, respectively) derived from the splitting of the $^3T_{2g}$ octahedral level in D_{4h} symmetry.[66,64] The 1.6 eV band and its shoulder at 1.66 eV are not at high enough energy to be the next spin-allowed d-d transitions, so we assign them as spin-forbidden transitions. This assignment is consistent with energies of the lowest D_{4h} split spin-forbidden (SF) transitions according to typical energy schemes of d^8 electron configurations in a D_{4h} crystal field.[82–85] Assignment of both bands as spin forbidden is supported by their identical field-dependent behavior, which points to a common electronic origin and with other evidence

from the H-dependent spectra, as will be discussed in Sec. III D. Although the intensity of the 1.58 and 1.60 eV ∥ and ⊥ bands is unexpectedly large for a spin-forbidden excitation, and may even exceed that of the neighboring spin-allowed bands (band overlap precludes determining the exact intensity of each), intensity borrowing between nearby spin-allowed and spin-forbidden bands is a well-known phenomenon[86] and can equalize the intensities of very close bands.[87,88] The SF bands, being d-d in origin, are electric-dipole forbidden as well as spin forbidden in an effective D_{4h} symmetry. Since the neighboring spin-allowed bands from which they borrow are vibronic in nature, an activated T-dependent behavior should also characterize the SF bands. This seems to be consistent with the increase in peak height of the 1.58 and 1.60 eV bands with increasing T, although it is difficult to separate out the T dependence of the SF bands and lower energy broad bands. In contrast, the 1.66 eV SF band follows the opposite trend with temperature, gaining somewhat in intensity as T decreases. We will address the question of SF band intensity again in Sec. III D.

Figure 5 displays the temperature-dependent visible region absorption bands in NENB for light polarized parallel and perpendicular to the chains. Similar broad bands appear in both polarizations, centered at about 2.55 eV (2.51 eV) in the ∥ (⊥) polarization. The ∥ polarized band is more intense and exhibits a weak 0.10 eV (800 cm^{-1}) vibrational progression on the lowest T spectrum. Both polarization bands increase in intensity slightly with temperature; the inset shows the T dependence of the intensities for the specified integration regions, after subtracting a flat absorption base line equal to α at the low energy side of the band. Neither T dependence is well fitted by $\coth(h\nu/kT)$ nor was the fit improved with other base lines. Compared to the NIR excitations which exhibit substantial T dependence, the degree of T dependence is much less in the visible absorption bands, suggesting that the majority of the band is T independent and originates from a dipole-allowed mechanism. Charge transfer (CT) transitions can be strongly allowed and have constant intensity over varying temperature,[64] so previous assignment[66] of this band in NENP as predominantly Ni^{2+}-to-NO_2^- charge transfer is consistent with its minimal T dependence. As noted previously, the band is rather weak for a CT transition and the low intensity may be due to limited overlap of the nitrite and Ni^{2+} orbitals.[89,90] The limited T dependence of the band may be due to some vibronic contribution to that overlap or to some underlying vibronic d-d band.

Assignment of the visible NENB band as charge transfer in nature is substantiated by our observation of the 800 cm^{-1} vibrational progression, not previously documented in NENP.[65] Several other complexes containing Ni^{2+} bound to NO_2^- through the nitrogen atom also have a band at about 2.5 eV, which has been assigned to a Ni^{2+}-to-NO_2^- π^* electron transfer transition.[64,90–94] That assignment was based on the low temperature appearance of a vibrational progression having a spacing of approximately 600 cm^{-1} in many of the spectra.[89,91,92] As pointed out by Finney *et al.*, such a frequency is too high to be a metal-ligand vibration but may be assigned to the deformation scissoring mode of the nitrite group.[91] Since the 600 cm^{-1} reported progression is substantially less than the 830 cm^{-1} vibrational frequency observed

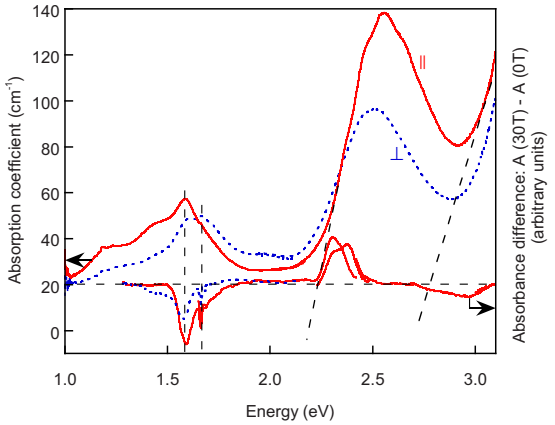

FIG. 6. (Color online) Overlay of the low T absorption coefficient (α) (upper two spectra) and the low T absorbance difference (AD) (lower two spectra) of NENB. The absorbance difference is the absorbance at high field H minus the absorbance at zero field (H=0 T). The vertical dashed lines highlight correspondences between the field-dependent AD and zero-field α features. Data from different samples in different spectral regions are normalized to the NIR data. Parallel (∥) and perpendicular (⊥) polarizations are shown by solid and dotted lines, respectively; no AD ⊥ polarized data are shown above 2 eV since no significant field-dependent features were found in that region. The scale of the AD spectra makes those feature sizes greatly exaggerated; AD features are actually only a 1%–2% of α. The AD=0 line is arbitrarily chosen to be at the level of the assumed α base line. The apparent double peak at ≈2.4 eV in the AD spectra shows a slight mismatch between data in different frequency regions taken on different samples.

for most NO_2^- complexes[95,96] and for the ground state of the free ion,[97] it was argued that the extra electron density in the antibonding excited state lowers the frequency of the vibration.[90,91] Such a frequency reduction has been observed in the vibrational progression on an internal nitrite excitation in sodium nitrite crystals.[97] In NENB and NENP, however, the weak progression on the CT band is reduced very little in frequency from the nitrite deformation frequencies at 816 and 875 cm^{-1} in the NENP vibrational spectrum.[48,78,98] Perhaps the delocalization of charge along the chain direction in NENB and NENP[48] makes the NO_2^- bridge deformation frequencies less susceptible to softening in the excited state. In any case, the obvious nitrite ion progression rules out the possibility that the 2.5 eV band is the second d-d transition localized on the Ni^{2+} ion. We do not assign this transition in the NENB spectrum; it is expected at approximately 2.2 eV, but may be obscured underneath the CT band or may be the weak band at 1.97 eV in the perpendicular polarization.[66]

D. Assignment of field-dependent absorption features

Figure 6 is an overlay of the NENB low temperature absorption coefficient α and the absorbance difference (AD) spectra at H=30 T. The two types of spectra are plotted on different scales and the AD features are highly exaggerated compared to α. Vertical dashed lines highlight corresponding features in the two types of measurements, thus revealing the nature of the field-dependent AD features based on our as-

signments of the zero-field spectrum. The excellent correspondence of NIR α and AD features indicates that the latter arise due to the field sensitivity of the spin-forbidden electronic excitations at 1.58, 1.60, and 1.66 eV. Furthermore, we see that these excitations are suppressed by high magnetic fields. The fine structure on the high energy sides of the NIR AD features is likely due to weak vibrational replicas of the SF bands, not observable in the zero-field absorption spectra. The 2.3 eV parallel polarized AD feature appears at the low energy onset of the CT band, so we assign it as the electronic origin of the Ni^{2+}-to-NO_2^- CT band. The CT band itself is broadened by NO_2^- vibrational progressions that do not appear in the field-dependent spectrum. In contrast to the SF excitations that are suppressed by field, the CT band increases in intensity with applied field. Finally, the AD feature at 3 eV is associated with a higher energy unidentified excitation, which may be either another charge-transfer transition (metal to ligand or ligand to metal) or an on-site Ni^{2+} *d-d* excitation.

Details of the AD spectra support our earlier assignment of the zero-field absorption bands at 1.58 ($\parallel$), 1.60 ($\perp$), and 1.66 eV ($\parallel$, $\perp$) as spin forbidden. A d^8 electron configuration in a D_{4h} crystal field has two spin singlet states, $^1A_{1g}$ and $^1B_{1g}$, derived from the octahedral ^1e_g level. In typical D_{4h} energy schemes,[82–85] the $^1A_{1g}$ level is at slightly lower energy than the $^1B_{1g}$ level, although in some schemes the levels are nearly degenerate[84] and in others the splitting of the singlet states is large (10^3 cm^{-1}).[82] The triplet-to-singlet $^3B_{1g}$-to-$^1B_{1g}$ transition is an example of a SF transition that is essentially a spin flip and thus is expected to have very narrow bandwidth,[64,87,90] since it involves no charge redistribution and thus no broadening due to atomic relocations.[99] The sharp spike at 1.66 eV in the AD spectrum is notable for the narrowness of its width, approximately 15 meV, and we assign it and the corresponding zero-field feature to the Ni^{2+} $^3B_{1g}$-to-$^1B_{1g}$ SF transition. Note that the field dependence gives a better indication of its actual spikelike shape, since in the absorption spectrum, it is largely obscured by overlapping nearby broad bands and is seen only as a tiny feature in Fig. 4. Since the $^3B_{1g}$-to-$^1B_{1g}$ SF transition includes a change of orbital symmetry, it is expected to be a broader band[99] than the $^3B_{1g}$-to-$^1B_{1g}$ transition. The bands at 1.58 and 1.60 eV in the $\parallel$ and $\perp$ polarizations are both broader and lower in energy than the 1.66 eV feature, so we assign these bands as the $^3B_{1g}$-to-$^1A_{1g}$ transition.

As mentioned above, the parallel polarization absorbance difference feature at 2.38 eV is located at the low energy onset of the 2.5 eV absorption band (Fig. 6). Although the latter zero-field band likely combines a weak vibronically induced *d-d* transition obscured by a dominant CT band, we assign the AD feature as due to the charge-transfer excitation for several reasons. First, the origin of the vibrational progressions on the CT band is located at 2.37 eV [Fig. 5(a)] in excellent agreement with the AD feature. Second, slight differences in the AD bands of NENP correlate well with differences in its zero-field CT bands.[74] Specifically, the energies of both the CT band and AD feature in NENP shift lower by 0.25 eV. In addition, NENP has a non-negligible AD band at similar energy in the perpendicular polarization, consistent with a much stronger CT band in the zero-field $\perp$ polarization.[74] Third, our comparative studies of paramagnetic analog materials also support this assignment. Of the two paramagnetic analog materials we have investigated, one compound contains NO_2^- groups bonded to the central Ni^{2+} through the N atom and it exhibits a similar zero-field CT band and AD band.[100] A second compound, NEN3P, lacks the CT band in both the zero-field and AD spectra, consistent with the absence of NO_2^- groups in its structure.

E. Comparison of $Ni(en)_2NO_2BF_4$ and a paramagnetic analog compound

$Ni(en)_3(ClO_4)_2 \cdot H_2O$ (NEN3P) contains isolated Ni^{2+} complexes separated by ClO_4^- counterions and an accompanying water molecule of crystallization in a loosely packed orthorhombic structure.[67] The Ni^{2+} ion is coordinated to the three en rings in approximately octahedral geometry, with the three chelating rings forming mutually perpendicular planes. Due to the high symmetry, no anisotropy is expected in the electronic excitations and our polarization tests confirmed negligible polarization dependence.

Figure 7 shows the NIR zero-field low *T* absorbance spectra of NEN3P and NENB overlaid with the 30 T AD spectra of the same two compounds. The AD spectra will be discussed in Sec. III F. The zero-field absorbance spectra are shown above the horizontal dashed line with NEN3P spectra in solid blue and NENB spectra in dotted red lines. The NEN3P spectrum is adjusted in height (by additive and multiplicative constants) to allow for easier comparison of features. Equivalent excitations in NEN3P and NENB are indicated by vertical dashed lines. The NIR spectrum of NEN3P is characteristic of octahedrally coordinated Ni^{2+}, having a single broad *d-d* band at 1.45 eV and a substantial rounded shoulder at 1.58 eV. These excitations have the same electronic origins as the equivalent energy excitations in NENB. The ligand field of the ethylenediamine rings determines the energy of the broad spin-allowed transition[66] and the 1.58 eV shoulder is the lowest *d-d* SF band. Missing in the NIR spectrum of NEN3P are the lower energy *d-d* band at about 1.25 eV and the second SF band at 1.66 eV seen in NENB. These are absent because the split *d* levels of D_{4h} symmetry are degenerate in O_h symmetry. All features in the NIR and visible spectrum of NEN3P increase in intensity with temperature, and the 1.58 eV shoulder persists to room temperature. In the visible frequency spectrum (not shown), NEN3P has a second *d-d* band at 2.32 eV, of similar intensity to the first *d-d* band, but it lacks the strong Ni^{2+}-to-NO_2^- CT band at about 2.5 eV, consistent with the absence of nitrite groups in the complex.

The mechanism by which spin-forbidden transitions become allowed is either through spin-orbit coupling or spin exchange.[101,102] In the case of spin-orbit (SO) coupling, intensity is gained by "borrowing" from nearby spin-allowed transitions of the same symmetry.[86] Due to mixing with nearby excited states, the pure spin nature of the forbidden state is not preserved and the selection rule no longer rigidly holds. The intensity gained in this way is proportional to the inverse square of the energy separation between the excited spin-forbidden and spin-allowed states.[86] Although by no

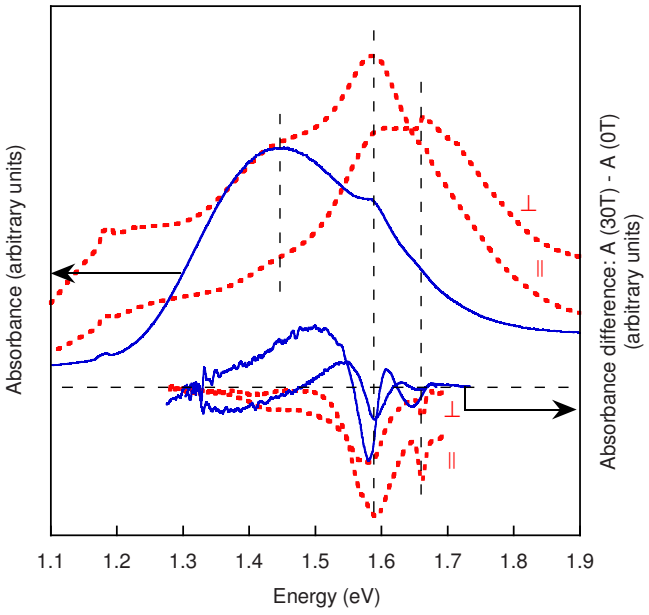

FIG. 7. (Color online) Overlay of the near infrared low T zero-field absorbance (upper spectra) and the low T absorbance difference at $H=30$ T (lower spectra) of NENB (dotted red lines) and NEN3P (solid blue lines). The absorbance difference (AD) is the absorbance at high field H minus the absorbance at zero field ($H=0$ T), taken at $T=4.2$ K. AD spectra of two different NEN3P samples are shown; the inconsistencies are discussed in the text (Secs. II and III E). NEN3P data are unpolarized, whereas NENB spectra are polarized perpendicular ($\perp$) or parallel ($\|$) to the chains. The absorbance of NEN3P is shifted and multiplied by a constant for easier comparison with that of NENB. The vertical dashed lines highlight similar features in the absorbance of the two compounds and the correspondence between field-dependent AD and zero-field absorbance features. Note that the scale of the AD spectra makes those feature sizes greatly exaggerated and the AD=0 line is chosen arbitrarily.

means universal, the appearance of SO-induced spin-forbidden transitions in Ni^{2+} spectra is not uncommon due to the significant spin orbit coupling of the Ni^{2+} ion.[87] In the case of a pairwise spin exchange mechanism, the nominally spin-forbidden excitations acquire significant intensity due to exchange interactions that couple pairs of metal ions or organic radicals. If the difference in total spin of the coupled ground and excited states is zero, then the transition is nominally allowed and can have the intensity of an allowed transition, depending on the strength of the exchange coupling.[101] Spin-exchange-induced SF transitions have been observed in compounds in which Ni^{2+} is coupled to transition metals or organic radicals,[103,104] with exchange values varying from approximately 20 to 200 cm^{-1}.

In materials such as NEN3P with noninteracting Ni^{2+} ions, the SF bands are induced by SO coupling. The close proximity of the spin-allowed and spin-forbidden bands in NEN3P makes the mixing mechanism for intensity borrowing possible and has been noted previously in other $Ni^{2+}(en)_3$ complexes.[87,105] In NENB, however, spin exchange produces the Haldane state and may also contribute to the SF band intensity. Figure 7 shows that the SF bands in NENB have much greater intensity relative to the spin-allowed bands than is true for the same bands in NEN3P. Since the energy separation of the spin-allowed and spin-forbidden bands is essentially identical in the two materials, the spin-orbit-induced SF intensity should also be identical. Thus, the evidence points to additional intensity enhancement of the 1.58 ($\|$) and 1.60 ($\perp$) eV excitations by spin exchange in NENB.[101,106] The 1.66 eV SF excitations, present only in NENB, may be activated solely by spin exchange, which is an efficient mechanism for allowing spin flip transitions.[101] The temperature dependence of a SF band can provide additional evidence to distinguish between a SO and exchange mechanism of intensity enhancement. The T-dependent behavior of the 1.58 and 1.60 eV bands is difficult to separate out from the rest of the d-d band and is inconclusive on this point. On the other hand, the 1.66 eV shoulder behavior is clear; the small shoulder is most pronounced at low T and gradually loses intensity until it disappears at $T \approx 200$ K in both polarizations. This behavior is opposite from that for intensity borrowing from a vibronic band but resembles the T dependence of a spin exchange mechanism in a bimetallic chain.[107] This provides further corroboration that the 1.66 eV shoulder is a spin-exchange-induced SF excitation. To confirm the mechanism, however, the exact T dependence of exchange-induced transitions in a Haldane chain should be calculated.

F. Field sensitivity of absorption intensities

In order to understand the field dependence of the electronic excitations, it is again useful to compare Haldane and paramagnetic compounds. The lower part of Fig. 7 compares the NIR AD features at $H=30$ T of NENB and NEN3P. Below or crossing the horizontal dashed line, the dotted red lines are the two AD polarizations of NENB and the solid blue lines are unpolarized AD spectra for two different NEN3P samples. Despite the inconsistencies discussed in Sec. II, the general AD features of the two NEN3P samples are similar enough to make a useful contrast to NENB, particularly in the vicinity of the SF band. Figure 8 shows the set of unpolarized NIR AD spectra for just one of the NEN3P samples. The inset shows the integrated intensities as a function of field for both samples; the integration region in both cases is the inverted SF-derived AD feature seen in Fig. 7 and is indicated in Fig. 8 by the double arrow. Again, there are some unexplained inconsistencies between NEN3P samples, but the SF band behavior is comparable and differs from that in NENB. One NEN3P sample has decreasing SF band intensity for all measured $H>0$ T, whereas the other sample appears to have significant intensity changes only above about 4 T; the change in slope near 4 T is more gradual than the intensity changes near the onset field in NENB, however, so we take an average NEN3P behavior as continuously changing from $H=0$ T. Note that none of the many measured NENB samples ever exhibited behavior close to that of the stronger H-dependent behavior of NEN3P in Fig. 8.

In paramagnetic NEN3P, the alternating positive and negative changes in the AD spectra (Figs. 7 and 8) suggest

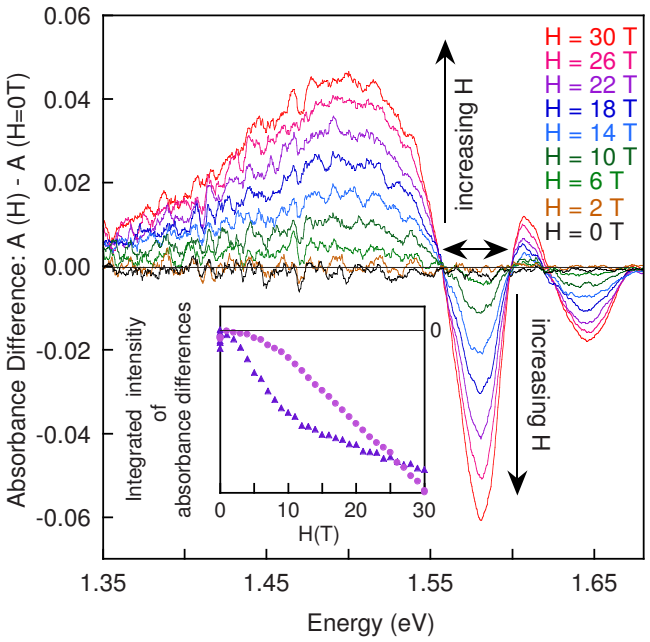

FIG. 8. (Color online) Near infrared absorbance difference spectra of single crystal NEN3P, of which the $H=30$ T AD spectrum is also shown in Fig. 7. The absorbance difference (AD) is the absorbance at high magnetic field (H) minus the absorbance at zero field ($H=0$ T). The field was applied parallel to the direction of light propagation (Faraday configuration) and the light was unpolarized. Spectra were taken at 1 T steps and repeated at $H=0$ T, after the field ramp was ramped down. The spectra are smoothed and shown only at selected field values, which are listed on the graph. The inset shows the integrated intensity (area under the curve, calculated from the unsmoothed data) of the absorbance difference as a function of field for two different samples of NEN3P; the inconsistencies are discussed in the text (Secs. II and III E) and can also be seen in the $H=30$ T AD spectra in Fig. 7. The integration region is indicated by a double arrow for this data set and is approximately the same for the other sample.

energy shifts of the SA and SF absorption bands, unlike the pure intensity effect observed in NENB (Fig. 1). Recall that the NENB SF band intensities decrease linearly with H but are unaffected by applied field for $H<H_{cr}$, just as the singlet ground state is essentially insensitive to field in the magnetization.[11] In contrast, the SF band in NEN3P responds immediately to applied field. As discussed in Sec. III E, the greater part of the SF intensity in NENB is probably induced by spin exchange, so the suppression of the SF intensity is therefore also likely due to a spin exchange effect. Basso calculated the probabilities of exchange-induced SF transitions of magnetic dopant ions in an AF lattice and found them to decrease in proportion to the square of the sublattice magnetization.[108] Although that finding is strongly configuration dependent and cannot be applied directly to our results, the relation to the magnetization is appealing since we also find a clear correlation between the SF band intensities and the high field magnetization, although in a linear dependence. We suggest that an extension of the method of Tanabe *et al.*[109] to the Haldane chain, in a manner similar to that done by Basso,[108] might be profitable to model our results.

The field-induced intensity changes of the 2.55 eV CT band in NENB are shown in the lower inset of Fig. 2, and these also evoke the magnetization of a Haldane system, with finite changes commencing only above H_{cr}. The mechanism of field sensitivity in the CT transition is likely different from that of the SF transition, however, due to the different electronic nature of the bands. In fact, field-sensitive CT transitions are also observed[100] in $Ni(tn)_2(NO_2)_2$ (tn =trimethylenediamine=$C_3N_2H_{10}$) (NTDN), another paramagnetic analog of NENB. NTDN has two NO_2^- groups bonded through N to the Ni^{2+} ion and exhibits the same Ni^{2+}-to-NO_2^- CT transition at $\approx$2.5 eV as seen in NENB. In NTDN, the CT band increases in intensity starting at $H=0$ T and appears to saturate above $H\approx 10$ T.[110] Thus, there exists the same contrasting behavior between the Haldane and paramagnetic compounds for the CT transition as for the SF band, with an onset at the crossover field being characteristic of the Haldane compound and continuous changes above $H=0$ T characterizing the paramagnet. Despite the distinct field dependencies, the existence of the same field-sensitive CT band in both NENB and NTDN suggests that the mechanism of field sensitivity is common to this particular Ni^{2+}-NO_2^- pairing. Viewed as a simple Ni^{2+}-to-NO_2^- electron transfer process (ignoring any aspect of covalency), the CT excitation changes both the spin and charge states of the two ions; spin-1 Ni^{2+} loses one of its two unpaired electrons and becomes Ni^{3+} with probable[111] spin state $S=1/2$, while the neighboring nitrite ion gains an unpaired electron. The excited charge-transfer state of Ni^{3+}-NO_2^{2-} may thus be affected by pairwise spin exchange. If the transferred electron in NENB is delocalized along the chain, however, as suggested in Sec. III C, the pairwise effect might be minimal. We find that the mechanism by which the Ni^{2+}-to-NO_2^- CT band gains intensity in an applied field is still unclear and merits further study.

To summarize, the Haldane compounds NENB, NENP, and some paramagnetic analog compounds have at least two different electronic excitations that are sensitive to applied magnetic field: the Ni^{2+} spin-forbidden d-d transition and the Ni^{2+}-to-NO_2^- CT transition. The characteristic response to magnetic field of the SF excitation depends on the mechanism by which it becomes allowed, spin exchange or spin-orbit coupling. The CT band, on the other hand, seems to have the same type of field sensitivity in both Haldane and paramagnetic materials. For the paramagnetic compounds, the changes in either band commence essentially at zero field, consistent with the response of isolated spins to any finite field, whereas for the Haldane compounds, there is an onset of changes that coincides with the crossover from low-field to high-field state. Thus, the details of the field dependence reflect the magnetic properties of the system, in particular, the high field magnetization.[11,12] (In contrast, the reopening of a field-induced gap[22,57] in NENB due to the staggered g tensor[55] is not revealed in the electronic band intensities.) We would expect to see similar correlation between the H-dependent electronic intensities and magnetization behaviors of other types of spin-gapped materials, but this remains to be investigated.

IV. CONCLUSION

We have investigated the temperature and field dependences of the optical properties of the Haldane compound, $Ni(en)_2NO_2BF_4$ (NENB). We have assigned near infrared spin-allowed and spin-forbidden *d-d* transitions of the Ni^{2+} ion as well as a Ni^{2+}-to-NO_2^- charge-transfer band, the latter confirmed by vibrational fine structure of the nitrite group. From a comparison with the paramagnetic analog compound, $Ni(en)_3(ClO_4)_2 \cdot H_2O$ (NEN3P), which has a similar but weaker SF transition, we conclude that spin exchange contributes intensity to the NENB SF excitations, in particular, to the sharp spin flip SF transition at 1.66 eV in both polarizations. The SF and CT transitions in NENB are both field dependent with intensity changes commencing only above the crossover field H_{cr}; the SF transition is diminished in strength by field, whereas the CT intensity is enhanced. The same transitions are field dependent in paramagnetic analog compounds, but with intensity changes occurring continuously above $H=0$ T. The details of the field sensitivity thus correlate strongly with the magnetic properties, in particular, with the high field magnetization.

ACKNOWLEDGMENTS

Thanks to D. Allen of Colby College who assisted by cleaving a large polycrystalline NENB sample into small single crystals, to D. Hall at NHMFL for his expertise on vibrating sample magnetometer magnetization measurements, to L. Balicas at NHMFL for help with cantilever magnetization measurements, and to A. Cornia for helpful comments on some of this work. The high magnetic field measurements were done at the National High Magnetic Field Laboratory in Tallahasee, FL, which is supported by NSF Cooperative Agreement No. DMR-0084173, by the State of Florida, and by the DOE. V.C.L., Y.-H.C., I.A.C., A.C.K., and J.R.M. acknowledge financial support from the Colby College Natural Science Division, Colby College Students' Special Projects Fund, and the Henry Luce Foundation.

*vclong@colby.edu

[1] J. P. Renard, L. P. Regnault, and M. Verdaguer, in *Magnetism: Molecules to Materials*, edited by J. S. Miller and M. Drillon (Wiley-VCH, New York, 2001), Vol. 1, pp. 49–93.
[2] A. Zheludev, S. Maslov, T. Yokoo, S. Raymond, S. E. Naglan, and J. Akimitsu, J. Phys.: Condens. Matter **13**, R525 (2001).
[3] K. Katsumata, High Magnetic Fields **2**, 171 (2003).
[4] F. D. M. Haldane, Phys. Rev. Lett. **50**, 1153 (1983).
[5] M. P. Nightingale and H. W. J. Blöte, Phys. Rev. B **33**, 659 (1986).
[6] M. Takahashi, Phys. Rev. Lett. **62**, 2313 (1989).
[7] I. Affleck, T. Kennedy, E. H. Lieb, and H. Tasaki, Phys. Rev. Lett. **59**, 799 (1987).
[8] W. J. L. Buyers, R. M. Morra, R. L. Armstrong, M. J. Hogan, P. Gerlach, and K. Hirakawa, Phys. Rev. Lett. **56**, 371 (1986).
[9] J. P. Renard, M. Verdaguer, L. P. Regnault, W. A. C. Erkelens, J. Rossat-Mignod, and W. G. Stirling, Europhys. Lett. **3**, 945 (1987).
[10] M. Yamashita, T. Ishii, and H. Matsuzaka, Coord. Chem. Rev. **198**, 347 (2000).
[11] K. Katsumata, H. Hori, T. Takeuchi, M. Date, A. Yamagishi, and J. P. Renard, Phys. Rev. Lett. **63**, 86 (1989).
[12] Y. Ajiro, T. Goto, H. Kikuchi, T. Sakakibara, and T. Inami, Phys. Rev. Lett. **63**, 1424 (1989).
[13] T. Takeuchi, H. Hori, T. Yosida, A. Yamagishi, K. Katsumata, J.-P. Renard, V. Gadet, M. Verdaguer, and M. Date, J. Phys. Soc. Jpn. **61**, 3262 (1992).
[14] G. E. Granroth, L.-K. Chou, W. W. Kim, M. Chaparala, M. J. Naughton, E. Haanappel, A. Lacerda, D. Rickel, D. R. Talham, and M. W. Meisel, Physica B **211**, 208 (1995).
[15] J. B. Parkinson and J. C. Bonner, Phys. Rev. B **32**, 4703 (1985).
[16] T. Sakai and M. Takahashi Phys. Rev. B **43**, 13383 (1991).
[17] J. P. Renard, V. Gadet, L. P. Regnault, and M. Verdaguer, J. Magn. Magn. Mater. **90-91**, 213 (1990).
[18] T. M. Brill, J. P. Boucher, L. C. Brunel, J. P. Renard, and M. Verdaguer, Physica B **204**, 303 (1995).
[19] L. C. Brunel, T. M. Brill, I. Zaliznyak, J. P. Boucher, and J. P. Renard, Phys. Rev. Lett. **69**, 1699 (1992).
[20] W. Lu, J. Tuchendler, M. von Ortenberg, and J. P. Renard, Phys. Rev. Lett. **67**, 3716 (1991).
[21] S. Luther, M. von Ortenberg, J. Tuchendler, and J. P. Renard, Physica B **211**, 213 (1995).
[22] M. Sieling, U. Löw, B. Wolf, S. Schmidt, S. Zvyagin, and B. Lüthi, Phys. Rev. B **61**, 88 (2000).
[23] L. P. Regnault, I. Zaliznyak, J. P. Renard, and C. Vettier, Phys. Rev. B **50**, 9174 (1994).
[24] I. A. Zaliznyak, D. C. Dender, C. Broholm, and D. H. Reich, Phys. Rev. B **57**, 5200 (1998).
[25] G. Xu, J. F. DiTusa, T. Ito, K. Oka, H. Takagi, C. Broholm, and G. Aeppli, Phys. Rev. B **54**, R6827 (1996).
[26] A. Zheludev, T. Masuda, I. Tsukada, Y. Uchiyama, K. Uchinokura, P. Böni, and S.-H. Lee, Phys. Rev. B **62**, 8921 (2000).
[27] Z. Honda, K. Katsumata, H. A. Katori, K. Yamada, T. Ohishi, T. Manabe, and M. Yamashita, J. Phys.: Condens. Matter **9**, L83 (1997).
[28] Z. Honda, H. Asakawa, and K. Katsumata, Phys. Rev. Lett. **81**, 2566 (1998).
[29] Z. Honda, K. Katsumata, M. Hagiwara, and M. Tokunaga, Phys. Rev. B **60**, 9272 (1999).
[30] Y. Chen, Z. Honda, A. Zheludev, C. Broholm, K. Katsumata, and S. M. Shapiro, Phys. Rev. Lett. **86**, 1618 (2001).
[31] A. Zheludev, Z. Honda, C. L. Broholm, K. Katsumata, S. M. Shapiro, A. Kolezhuk, S. Park, and Y. Qiu, Phys. Rev. B **68**, 134438 (2003).
[32] A. Zheludev, S. M. Shapiro, Z. Honda, K. Katsumata, B. Grenier, E. Ressouche, L.-P. Regnault, Y. Chen, P. Vorderwisch, H.-J. Mikeska, and A. K. Kolezhuk, Phys. Rev. B **69**, 054414 (2004).
[33] A. Zheludev, B. Grenier, E. Ressouche, L.-P. Regnault, Z. Honda, and K. Katsumata, Phys. Rev. B **71**, 104418 (2005).
[34] L. P. Regnault and J. P. Renard, Physica B **234-236**, 541 (1997).

[35] M. Chiba, T. Fukui, Y. Ajiro, M. Hagiwara, T. Goto, and T. Kubo, Physica B **246-247**, 576 (1998).
[36] S. A. Zvyagin, in *Spectroscopy of Emerging Materials*, edited by E. C. Faulques (Kluwer Academic, Dordrecht, 2004), Vol. 1, pp. 239–250.
[37] T. Ito, H. Yamaguchi, K. Oka, K. M. Kojima, H. Eisaki, and S. Uchida, Phys. Rev. B **64**, 060401(R) (2001).
[38] Y. Fagot-Revurat, D. Malterre, F.-X. Lannuzel, E. Janod, C. Payen, L. Gavioli, and F. Bertran, Phys. Rev. B **67**, 125118 (2003).
[39] M. N. Popova, S. A. Klimin, E. P. Chukalina, E. A. Romanov, B. Z. Malkin, E. Antic-Fidancev, B. V. Mill, and G. Dhalenne, Phys. Rev. B **71**, 024414 (2005).
[40] M. N. Popova, S. A. Klimin, E. P. Chukalina, B. Z. Malkin, R. Z. Levitin, B. V. Mill, and E. Antic-Fidancev, Phys. Rev. B **68**, 155103 (2003).
[41] J. F. DiTusa, S.-W. Cheong, J.-H. Park, G. Aeppli, C. Broholm, and C. T. Chen, Phys. Rev. Lett. **73**, 1857 (1994).
[42] K. Maiti and D. D. Sarma, Phys. Rev. B **58**, 9746 (1998).
[43] R. Rückamp *et al.*, New J. Phys. **7**, 144 (2005).
[44] J. Ferré, J. P. Jamet, C. P. Landee, K. A. Reza, and J. P. Renard, J. Phys. (France) **49**, 1441 (1988).
[45] T. Ishii, N. Aizawa, H. Hara, M. Yamashita, and H. Matsuzaka, Polyhedron **20**, 1297 (2001).
[46] A. Meyer, A. Gleizes, J. Girerd, M. Verdaguer, and O. Kahn, Inorg. Chem. **21**, 1729 (1982).
[47] M. G. B. Drew, D. M. L. Goodgame, M. A. Hitchman, and D. Rogers, Chem. Commun. (London) **20**, 477 (1965).
[48] B. J. Hathway and R. C. Slade, J. Chem. Soc. A **1967**, 952 (1967).
[49] C. P. Landee, K. A. Reza, M. R. Bond, and R. D. Willett, Phys. Rev. B **56**, 147 (1997).
[50] Single crystal x-ray data of NENB taken at 113 K are deposited in the Cambridge database, CCDC 638437.
[51] J. P. Renard, M. Verdauer, L. P. Regnault, W. A. C. Erkelens, J. Rossat-Mignod, J. Ribas, W. G. Stirling, and C. Vettier, J. Appl. Phys. **63**, 3538 (1988).
[52] O. Avenel *et al.*, Phys. Rev. B **46**, 8655 (1992).
[53] M. Hagiwara, K. Katsumata, I. Affleck, B. I. Halperin, and J. P. Renard, Phys. Rev. Lett. **65**, 3181 (1990).
[54] S. H. Glarum, S. Geschwind, K. M. Lee, M. L. Kaplan, and J. Michel, Phys. Rev. Lett. **67**, 1614 (1991).
[55] M. Chiba, Y. Ajiro, H. Kikuchi, T. Kubo, and T. Morimoto, Phys. Rev. B **44**, 2838 (1991).
[56] P. P. Mitra and B. I. Halperin, Phys. Rev. Lett. **72**, 912 (1994).
[57] T. Sakai and H. Shiba, J. Phys. Soc. Jpn. **63**, 867 (1994).
[58] T. C. Kobayashi, Y. Tabuchi, K. Amaya, Y. Ajiro, T. Yosida, and M. Date, J. Phys. Soc. Jpn. **61**, 1772 (1992).
[59] T. Manabe *et al.*, Synth. Met. **116**, 415 (2001).
[60] M. Hagiwara, K. Katsumata, H. Hori, T. Takeuchi, M. Date, A. Yamagishi, J. P. Renard, and I. Affleck, Physica B **177**, 386 (1992).
[61] T. C. Kobayashi, H. Honda, A. Koda, and K. Amaya, J. Phys. Soc. Jpn. **64**, 2609 (1995).
[62] M. Hagiwara, K. Katsumata, S. Sasaki, N. Narita, I. Yamada, and T. Yosida, J. Phys. Soc. Jpn. **64**, 3647 (1995).
[63] M. Hagiwara and K. Katsumata, J. Phys. Soc. Jpn. **61**, 1481 (1992).
[64] A. B. P. Lever, *Inorganic Electronic Spectroscopy*, 2nd ed. (Elsevier, Amsterdam, 1984).
[65] I. M. Walker, A. B. P. Lever, and P. J. McCarthy, Can. J. Chem. **58**, 823 (1980).
[66] A. J. Finney, M. A. Hitchman, C. L. Raston, G. L. Rowbotton, and A. H. White, Aust. J. Chem. **34**, 2159 (1981).
[67] C. L. Raston, A. H. White, and A. C. Willis, Aust. J. Chem. **31**, 415 (1978).
[68] Since our polarization tests were confined to rotations within the plane of a single sample, some unrecognized polarization dependence is possible.
[69] The conditions for stability of NEN3P samples were not fully determined. Some samples became opaque very quickly after gluing to a sample holder, whereas others lost only a little translucency and regained it in vacuum.
[70] M. Fox, *Optical Properties of Solids* (Oxford University Press, New York, 2001).
[71] We recalculated α using the more complete expression for the transmittance (Ref. 70), $\mathrm{Tr}=(1-R)^2\exp(-\alpha t)$, where R is the measured reflectivity (ideally of an opaque sample) and t is the transmitting sample thickness. Since our reflectance sample was not fully opaque, the measured R may be less than the actual reflectivity. Even allowing for reflectivities as high as 10%, the absorption coefficient changes [shifts downward by the small constant $-2\ln(1-R)$] by less than 5%.
[72] Samples with cleaved flat reflective surfaces gave greater values of α than samples with as-grown poorly reflective surfaces, consistent with the more complete expression for the transmittance (Ref. 71).
[73] NIR electronic absorption bands extend down to about 0.84 eV before the spectrum flattens out.
[74] V. C. Long, X. Wei, M. M. Turnbull, and C. P. Landee, National High Magnetic Field Laboratory 2003 Annual Research Review (unpublished), http://www.magnet.fsu.edu/usershub/publications/annualreportsearch.aspx?y=2003&p=3&id=L
[75] V. C. Long, P. O. Makumbe, E. C. Schundler, K. R. Maxcy, B. R. Landry, M. M. Turnbull, and C. P. Landee (unpublished).
[76] S. A. Zvyagin, B. R. Landry, and M. M. Turnbull (unpublished).
[77] B. Henderson and G. F. Imbusch, *Optical Spectroscopy of Inorganic Solids*, 1st ed. (Clarendon, Oxford/Oxford University Press, New York, 1989).
[78] W. Lu, M. von Ortenberg, J. Tuchendler, J. P. Renard, O. Neumann, and R. Geick, Chin. Phys. Lett. **10**, 695 (1993).
[79] V. C. Long, M. Kapoor, E. C. Schundler, K. R. Maxcy, B. R. Landry, M. M. Turnbull, and C. P. Landee (unpublished).
[80] We measured slightly different low T band shapes for NENP compared to the published spectra of Ref. 65 in the NIR region. This is likely due to leakage of our polarizer in that region, as mentioned in Sec. II.
[81] A. Takeuchi, K. Sato, K. Sone, S. Yamada, and K. Yamasaki, Inorg. Chim. Acta **1**, 399 (1967).
[82] M. A. Hitchman, Inorg. Chem. **11**, 2387 (1972).
[83] P. L. Meredith and R. A. Palmer, Inorg. Chem. **10**, 1049 (1971).
[84] D. A. Rowley and R. S. Drago, Inorg. Chem. **6**, 1092 (1967).
[85] A. F. Schreiner and D. J. Hamm, Inorg. Chem. **12**, 2037 (1973).
[86] C. J. Ballhausen, *Molecular Electronic Structures of Transition Metal Complexes*, 1st ed. (McGraw-Hill, London, 1979).
[87] B. N. Figgis and M. A. Hitchman, *Ligand Field Theory and Its Applications*, 1st ed. (Wiley-VCH, New York, 2000).
[88] H. Ito and K. Sone, Bull. Chem. Soc. Jpn. **58**, 2703 (1985).
[89] A. J. Finney, M. A. Hitchman, C. L. Raston, G. L. Rowbotton, and A. H. White, Aust. J. Chem. **34**, 2069 (1981).

[90] M. A. Hitchman and G. L. Rowbottom, Coord. Chem. Rev. **42**, 55 (1982).
[91] A. J. Finney, M. A. Hitchman, C. L. Raston, G. L. Rowbottom, and A. H. White, Aust. J. Chem. **34**, 2085 (1981).
[92] A. J. Finney, M. A. Hitchman, C. L. Raston, G. L. Rowbotton, and A. H. White, Aust. J. Chem. **34**, 2125 (1981).
[93] A. J. Finney, M. A. Hitchman, C. L. Raston, G. L. Rowbotton, and A. H. White, Aust. J. Chem. **34**, 2139 (1981).
[94] A. J. Finney, M. A. Hitchman, C. L. Raston, G. L. Rowbotton, and A. H. White, Aust. J. Chem. **34**, 2047 (1981).
[95] K. Nakamoto, J. Fujita, and H. Murata, J. Am. Chem. Soc. **80**, 4817 (1958).
[96] K. Nakamoto, *Infrared and Raman Spectra of Inorganic and Coordination Compounds: Part B*, 5th ed. (Wiley, New York, 1997).
[97] J. Sidman, J. Am. Chem. Soc. **79**, 2668 (1957).
[98] D. M. L. Goodgame, M. A. Hitchman, and D. F. Marsham, J. Chem. Soc. A **1971**, 259 (1971).
[99] D. Sutton, *Electronic Spectra of Transition Metal Complexes*, 1st ed. (McGraw-Hill, London, 1968).
[100] V. C. Long, A. C. Kozen, J. R. Montague, X. Wei, B. R. Landry, M. M. Turnbull, and C. P. Landee, National High Magnetic Field Laboratory 2005 Research Report (unpublished), http://www.magnet.fsu.edu/mediacenter/publications/reports/2005annualreport/2005-NHMFL-Report264.pdf
[101] H. U. Güdel, in *Magneto-Structural Correlations in Exchange Coupled Systems*, edited by R. D. Willett, D. Gatteschi, and O. Kahn (Reidel, Boston, 1985), pp. 297–327.
[102] P. McCarthy and H. U. Güdel, Coord. Chem. Rev. **88**, 69 (1988).
[103] J. Ferguson, H. J. Guggenheim, and Y. Tanabe, J. Chem. Phys. **45**, 1134 (1966).
[104] T. Yoshida, T. Suzuki, K. Kanamori, and S. Kaizaki, Inorg. Chem. **38**, 1059 (1999).
[105] C. K. Jørgensen, Acta Chem. Scand. (1947-1973) **9**, 1362 (1955).
[106] O. S. Wenger and H. U. Güdel, Inorg. Chem. **40**, 157 (2001).
[107] O. Cador, C. Mathonière, and O. Kahn, Inorg. Chem. **39**, 3799 (2000).
[108] H. C. Basso, Phys. Rev. B **56**, 9181 (1997).
[109] Y. Tanabe, T. Moriya, and S. Sugano, Phys. Rev. Lett. **15**, 1023 (1965).
[110] V. C. Long, A. C. Kozen, J. R. Montague, E. C. Schundler, P. O. Makumbe, X. Wei, B. R. Landry, K. R. Maxcy, M. M. Turnbull, and C. P. Landee, Proceedings of the Tenth International Conference on Molecule-Based Magnets (unpublished), http://www.icmm2006.uvic.ca/
[111] S. Collinson and M. Schröder, in *Advanced Inorganic Chemistry*, 6th ed., edited by F. A. Cotton, G. Wilkinson, and C. A. Murillo (Wiley, New York, 1999), pp. 1–32.